UNIVERSITY OF BIRMINGHAM

Research at Birmingham

Vibrational and electronic excitations in fluorinated ethene cations from the ground up

Harvey, Jonelle; Hemberger, Patrick; Bodi, Andras; Tuckett, Richard

Link to publication on Research at Birmingham portal

Vibrational and electronic excitations in fluorinated ethene cations from the ground up

Jonelle Harvey,[1] Patrick Hemberger,[2,a)] Andras Bodi,[2] and Richard P. Tuckett[1,a)]

[1]*School of Chemistry, University of Birmingham, Edgbaston, Birmingham B15 2TT, United Kingdom*
[2]*Molecular Dynamics Group, Swiss Light Source, Paul Scherrer Institut, Villigen CH 5232, Switzerland*

Valence threshold photoelectron spectra of four fluorinated ethenes; C_2H_3F, 1,1-$C_2H_2F_2$, C_2HF_3, and C_2F_4 were recorded at the Swiss Light Source with 0.002 eV resolution. The adiabatic ionization energies were found to be 10.364 ± 0.007, 10.303 ± 0.005, 10.138 ± 0.007, and 10.110 ± 0.009 eV, respectively. The electronic ground state of each cation shows well-resolved multi-component vibrational progressions, the dominant transitions being in the C=C stretching mode. Density functional theory based Franck–Condon simulations are used to model the vibrational structure and assign the spectra, sometimes revising previous assignments. An additional vibrational progression in the first photoelectron band of 1,1-$C_2H_2F_2$ indicates that the ground electronic state of the molecular ion is no longer planar. It is shown that *ab initio* vibrational frequencies together with the observed vibrational spacings do not always suffice to assign the spectra. In addition to symmetry rules governing the transitions, it is often essential to consider the associated Franck–Condon factors explicitly. Ionization to higher lying excited valence electronic states were also recorded by threshold ionization up to 23 eV photon energy. Equation-of-motion coupled cluster with single and double substitutions for ionization potential (EOM-IP-CCSD/cc-pVTZ) calculations confirmed historic electronic state assignments, and untangled the ever more congested spectra with increasing F-substitution. Previous attempts at illuminating the intriguing dissociative photoionization mechanism of fluorinated ethenes are reconsidered in view of new computational and experimental results. We show how non-statistical F-atom loss from $C_2H_3F^+$ is decoupled from the ground state dissociation dynamics in the energy range of its $\tilde{C}$ state. Both the statistical and the non-statistical dissociation processes are mediated by a plethora of conical intersections. © *2013 American Institute of Physics*. [http://dx.doi.org/10.1063/1.4795428]

I. INTRODUCTION

The perfluoro effect, i.e., π orbital destabilization with respect to σ orbitals, is observed when substituting hydrogen atoms with fluorine atoms in the series of molecules ranging from ethene to tetrafluoroethene.[1,2] The earliest comprehensive study of the ionization properties of fluorinated ethene molecules was reported by Sell and Kuppermann,[3] who studied the photoelectron angular distributions in the ground and excited state bands of the HeI photoelectron spectra (PES) of $C_2H_{4-n}F_n$ ($n = 0–4$) molecules. The HeII PES have been recorded and interpreted, among others, by Bieri *et al.*[1] with many body Green's function calculations. The Franck–Condon factors for the vibrational progressions in the ground state PES bands of C_2H_3F, 1,1-$C_2H_2F_2$, and C_2HF_3 were calculated by Takeshita,[4] based on Hartree–Fock geometries and force constant matrices. However, he did not attempt to compare the theoretical spectra with experiment. High resolution HeI PES and slightly lower resolution threshold photoelectron spectra (TPES) of C_2H_3F and 1,1-$C_2H_2F_2$ have been reported recently by Locht *et al.*[5,6] along with *ab initio* calculations. The latest HeII photoelectron spectrum

of C_2HF_3 was recorded by Bieri *et al.*[1] in 1981, but neither a high resolution HeI PES nor a TPES has been reported since. The TPES of C_2F_4, recorded by Jarvis *et al.*,[7] significantly improved upon the resolution of the early work by Sell and Kuppermann.[3] Lately, the HeI PES of C_2F_4 has been studied by Eden *et al.*,[8] with an even higher resolution and signal-to-noise ratio.

We recently studied the dissociative photoionization dynamics of the four aforementioned fluoroethenes.[9] The first dissociative photoionization channel opens up in a Franck–Condon gap above the electronic ground state $\tilde{X}$. We also found that F-atom loss is initially a statistical process in three of the four molecular ions, the exception being tetrafluoroethene. It then turns into a largely non-statistical process at higher energies. We based this conclusion predominantly on the correlation of the F-loss fragment ion signal with features of the TPES, indicating isolated state behaviour, in agreement with previous observations.[10–13] However, we also found that the internal energy distribution of the F-loss daughter ion $C_2F_3^+$ from $C_2F_4^+$ can be modelled assuming a purely statistical dissociation on the $\tilde{A}$ electronic state of the parent ion,[9] contrary to previous reports which invoked impulsive processes.[7]

In this work, we report the high resolution TPES of the first photoelectron band of these four molecules, i.e.,

a)Authors to whom correspondence should be addressed. Electronic addresses: patrick.hemberger@psi.ch and r.p.tuckett@bham.ac.uk.

ionization to the ground electronic state of the cation. Excited vibrational states are observed with particular clarity and Franck–Condon simulations are employed to assign vibrational progressions. This method has successfully been employed in the study of the photoelectron spectra of small systems, e.g., vinyl alcohol[14] and much larger molecules such as ovalene, $C_{32}H_{14}$,[14] as well as for interstellar carbenes[15] and diradicals.[16] The simulations are based upon density functional theory (DFT) geometries and Hessians of the neutral molecule and the cation. This goes beyond the cursory assignment based on vibrational spacings and calculated frequencies. Not only do Franck–Condon factors include symmetry considerations per se, they also indicate the relative intensities and the band profile based on the predicted geometry change. This can be vitally important in resolving ambiguities for modes with similar frequencies, or for near degenerate vibrational states. Franck–Condon fits based on DFT force constants are also used to study the parent ion geometries with respect to the *in silico* geometry optimization results. Of particular interest is any loss in planarity of the molecule upon ionization. If the C_S symmetry is conserved and the geometry change is small, only totally symmetric vibrational transitions are allowed in photoionization. However, if the cation becomes non-planar, other vibrational transitions can also gain intensity and become observable. This is indeed the case for $C_2H_4^+$, where the ground state ion tunnels through the barrier of planarity to a torsional (dihedral) angle of 29.2°.[17] In this instance, odd quanta of the non-symmetric twist-assisted mode v_4 are given intensity due to vibronic coupling between the $\tilde{X}$ and $\tilde{A}$ cation electronic states.[18] *Ab initio* calculations suggest that all four molecules remain planar upon ionization, but when Franck–Condon factors are considered, loss of planarity is discovered for 1,1-$C_2H_2F_2$ as a result of ionization from the C=C double bond. The successful application of fitting the ground state band with the Franck–Condon intensities and apparent similarities between the PES[1,3,5,6] and TPES of this work indicates that no autoionization effects are seen. Locht *et al.*[5,6] reported a large intensity ratio for the excited vs. ground electronic state bands in the TPES, whereas we find that the ground state bands have comparable intensities to the first excited state band in the TPES. This could be due to disparities between how the photon flux is accounted for.

With increasing F-substitution, the excited states become more indiscernible in the TPES. This spectral congestion may lead one to assume that electronically excited state assignments are fraught with dangers. However, Koopmans' theorem holds and our coupled-cluster assignments agree very well with earlier Hartree–Fock calculations.[1] Two further aspects of the electronically excited states are also touched on. First, we tentatively assign vibrational structures observed in the TPES of excited states. Second, the nature and role of the excited states with regard to the various dissociation pathways has been probed. Specifically, we try to explain the mechanism of non-statistical F-loss in the $\tilde{C}$ state band in the monofluoroethene cation observed in a previous study,[9] and aided by quantum chemical calculations, generalize it to other members of the fluorinated ethene series.

II. EXPERIMENTAL AND THEORETICAL METHODS

A. Experimental

Experiments were performed on the vacuum ultraviolet (VUV) beamline of the Swiss Light Source (SLS) at the Paul Scherrer Institut in Villigen, Switzerland. The synchrotron radiation is dispersed by a grazing-incidence plane-grating monochromator with 600 and 1200 mm^{-1} gratings. The ultimate resolving power of the monochromator is 10 000, i.e., 1 meV at 10 eV. Higher harmonic orders of the monochromatic radiation are suppressed with a compact rare gas filter operating at a pressure of 10 mbar.[19] The photon energy is calibrated in the first and second order against argon and neon autoionizing states.

The resident imaging photoelectron photoion coincidence (iPEPICO) spectrometer combines a Wiley–McLaren time-of-flight (TOF) mass spectrometer[20] and a velocity map imaging electron spectrometer. The pure sample was introduced into the chamber through an effusive source at room temperature, with typical pressures in the experimental chamber being $2–4 \times 10^{-6}$ mbar during measurement. The sample is ionized by the incident monochromatic VUV radiation. The photoelectrons are extracted by a continuous field and velocity map imaged onto a position sensitive delay line anode (Roentdek DLD40) with a kinetic energy resolution of 1 meV at threshold. Electrons with non-zero kinetic energy, the "hot" electrons, have a velocity vector that is oriented along the flight tube axis and also arrive at the centre of the detector along with the threshold electrons. The hot electron contamination of the threshold signal is removed by a subtraction process.[21] The resulting spectra were flux normalized using a sodium salicylate coated pyrex window with a photomultiplier tube. The ground electronic state spectrum of $C_2F_4^+$ was recorded at 20 V cm^{-1} and at 120 V cm^{-1} extraction fields. Based on a previous study of Ar, N_2, and CH_3I,[22] the threshold photoelectron peak positions could be expected to be Stark shifted[23] by 5 meV to lower energy when applying the higher field. In the same study,[22] field effects were found not to play a role in off-resonance threshold photoionization, which suggests that autoionization can compete effectively with field ionization in the absence of long-lived Rydberg states. In $C_2F_4^+$, the TPES peak positions did not shift measurably as a function of the field strength, indicating fast autoionization and neutral decay channels for high-n Rydberg states. Thus, the constant extraction field of 120 V cm^{-1} does not affect the TPES peak positions significantly in this polyatomic molecule. The error for both the adiabatic (AIE) and vertical (VIE) ionization energies were determined by taking the half width at half maximum of a Gaussian function fitted to the experimental spectrum.

B. Computational methods

Density functional theory (B3LYP/6-311++G(d,p)) calculations were performed using the GAUSSIAN 03 suite of programs to obtain the geometry and vibrational frequencies of the ground state neutral, as well as of the ground

state cation.[24] The Franck–Condon factors for photoionization to different vibrational levels of the electronic ground state of the cations were calculated using the program "FC-fit v2.8.8."[25] The first stage uses the optimized geometries for the neutral and cation, together with the *ab initio* force constant matrices, to calculate a stick spectrum, which helped to assign the peaks in the TPES. In the second stage, the relative intensities of the vibrational peaks in the major progression, the C=C stretching mode, are fitted by fine-tuning the cation geometry, followed by subsequent fitting of the intensities of the weaker progressions.[25] Finally, the stick spectrum is convoluted with a Gaussian function to simulate the rotational envelope and compare with experiment. Table S1 of the supplementary material[26] gives the structure and three sets of geometries for the four molecules under study. First, the B3LYP geometry of the neutral; second, the initial B3LYP geometry of the cation; and third, the final geometry of the cation obtained in the Franck–Condon fit. Vertical ionization energies were calculated at the G3B3[27] derived neutral geometries using equation-of-motion coupled-cluster for ionized states (EOM-IP-CCSD/cc-pVTZ) with the Q-Chem 3.2 program[28] (Table S2 of the supplementary material).[26]

III. RESULTS AND DISCUSSION

A. Ground electronic state of the cations

1. Monofluoroethene

The TPES of C_2H_3F and the simulated stick and convoluted spectra are shown in Figure 1(a). The HOMO (highest occupied molecular orbital) of the C_S symmetry neutral is the C=C π bonding orbital $(2a'')^2$, and the cation ground state has the term symbol $\tilde{X}\ ^2A''$. The geometry obtained from FC-fit shows that planarity is conserved upon ionization to the ground electronic state of the cation, however, the C=C bond length increases significantly from 1.320 to 1.409 Å, and the C–F bond length decreases from 1.354 to 1.274 Å. Removing an electron from the HOMO, of bonding character between the carbon atoms, leads to an increase in C=C bond length, whereas the C–F bond length decreases, because the HOMO has antibonding character between the carbon and fluorine atoms (see also the schematic structure at the bottom of Figure 4).

Our ground state TPES is in agreement with the lower resolution TPES recorded by Locht *et al.*[5] and it matches very well with the higher resolution HeI PES of the same
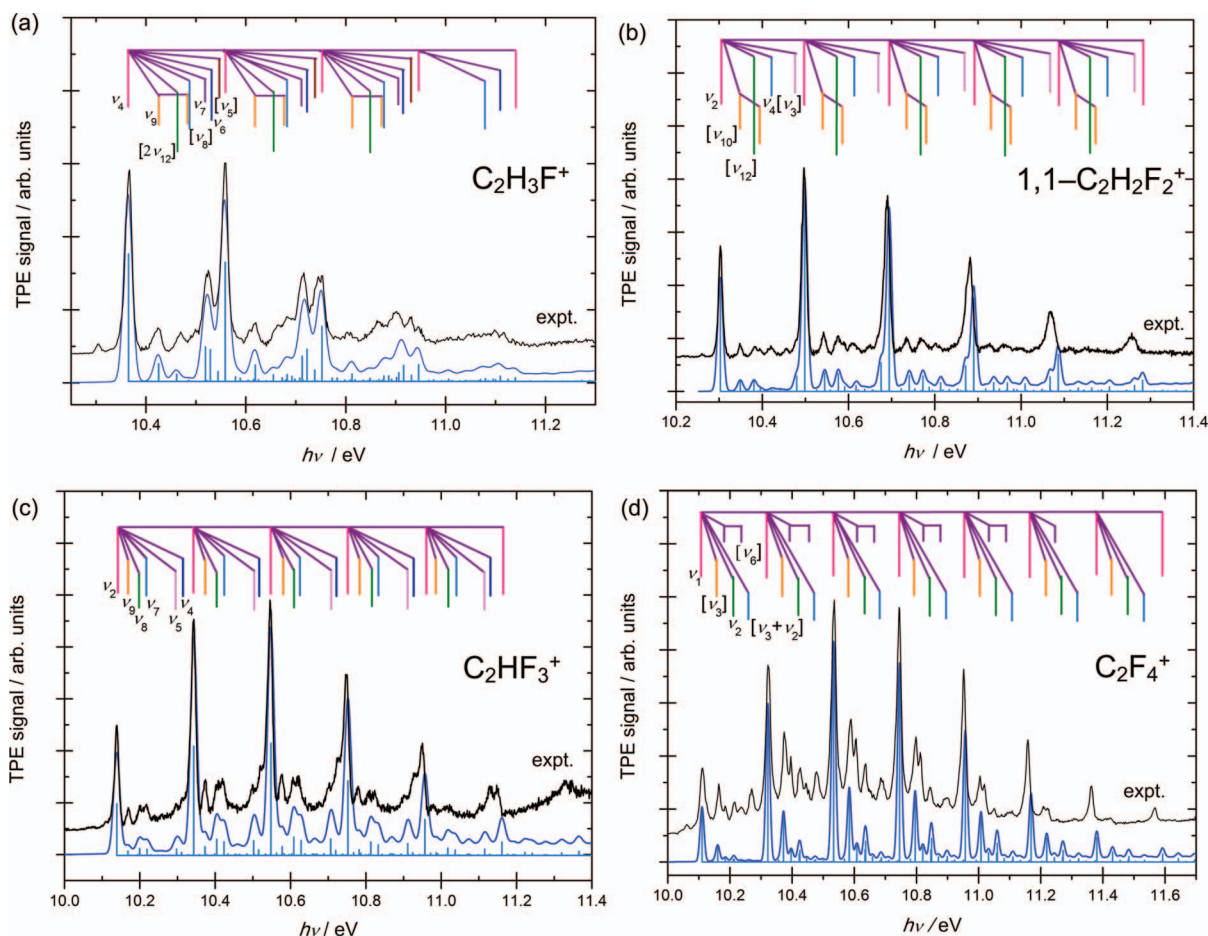

FIG. 1. The first TPES band of (a) C_2H_3F, (b) 1,1-$C_2H_2F_2$, (c) C_2HF_3 and (d) C_2F_4 is shown with the Franck–Condon stick (blue stick) simulations and convoluted curve (blue curves). Reassignments of vibrational modes are indicated by square brackets.

authors. The AIE is found to be 10.364 ± 0.007 eV and the VIE is 10.556 ± 0.007 eV, both in excellent agreement with previously reported values[5] of 10.363 ± 0.004 and 10.558 ± 0.004 eV, respectively. The *ab initio* frequencies together with observed frequencies and peak positions are given in Tables S3 and S4 of the supplementary material.[26]

The hot band at 10.304 eV most likely corresponds to $\nu_9'' = 1$, i.e., to the CHF=CH$_2$ wagging mode, calculated to be 484 cm^{-1}, comparing exactly with the experimental value of 0.062 eV or 484 cm^{-1}. We also note that the ν_9'' vibrational mode has a' symmetry and is totally symmetric. Similar to the work of Locht *et al.*,[5] we identify the major progression to be the ν_4 C=C stretching mode, with up to four quanta observed. The vibrational wavenumbers, symmetries, and descriptions of the modes Franck–Condon active upon ionization are given in Figure 2 and peak positions and assignments are shown in Figure 1(a). The harmonic frequency for this mode is determined by fitting the vibrational transitions ($\nu_4 = 0$–4) to a Morse potential thereby accounting for the anharmonicity, using the well-known[29] approximation $E(v+1) - E(v) = h\nu_0 - [(v+1)(h\nu_0)^2/2D_e]$ where $h\nu_0$ is the harmonic vibrational frequency and D_e is the dissociation energy.[9] The ν_4 harmonic frequency of 1552 cm^{-1} (Figure 2) is in excellent agreement with the B3LYP prediction of 1561 cm^{-1}. Discrepancies in the energies between the simulated and the experimental spectra towards higher eV are due to anharmonicity

which is disregarded in the harmonic model of FCfit. The anharmonicity constant, x_e, is determined to be 0.00514.

Aside from the ν_4 progression, some of our assignments of the remaining weak and complex progressions differ from those of Locht *et al.*[5,6] We agree with the assignment of the first peak to high energy of the origin band at 10.422 eV to be ν_9 of a' symmetry. However, the second peak at 10.468 eV is 0.102 eV (823 cm^{-1}) higher than the origin band, whilst the next member in the progression at 10.662 eV has a difference of 0.106 eV (855 cm^{-1}) from the $1\nu_4$ peak. The average of the two values is 839 cm^{-1}. We assign this peak to two quanta of the a'' symmetry ν_{12} mode, calculated at 389 cm^{-1}. Indeed, the intensities of $2\nu_{12}$ are well reproduced in the Franck–Condon simulation. Note that even-quanta transitions of non-totally symmetric modes are allowed, as a'' × a'' = a'. Locht *et al.*[5] assign this progression as one quantum of the ν_8 mode. This mode has the correct a' symmetry to be observed in odd quanta, but its calculated value at 981 cm^{-1} is significantly higher than the measured 839 cm^{-1} level spacing. The Franck–Condon simulation places this mode at a somewhat higher energy. We reassign all peaks previously attributed by Locht *et al.*[5] as $(n\nu_4 + \nu_8)$ to $(n\nu_4 + 2\nu_{12})$.

The next nearest peak towards the $\nu_4 = 1$ transition at 10.523 eV has been assigned by Locht *et al.*[5] to the ν_7 mode, a H$_a$–C=C scissor (where H$_a$ is the hydrogen *cis* to the fluorine, see Table S1 of the supplementary material).[26] The
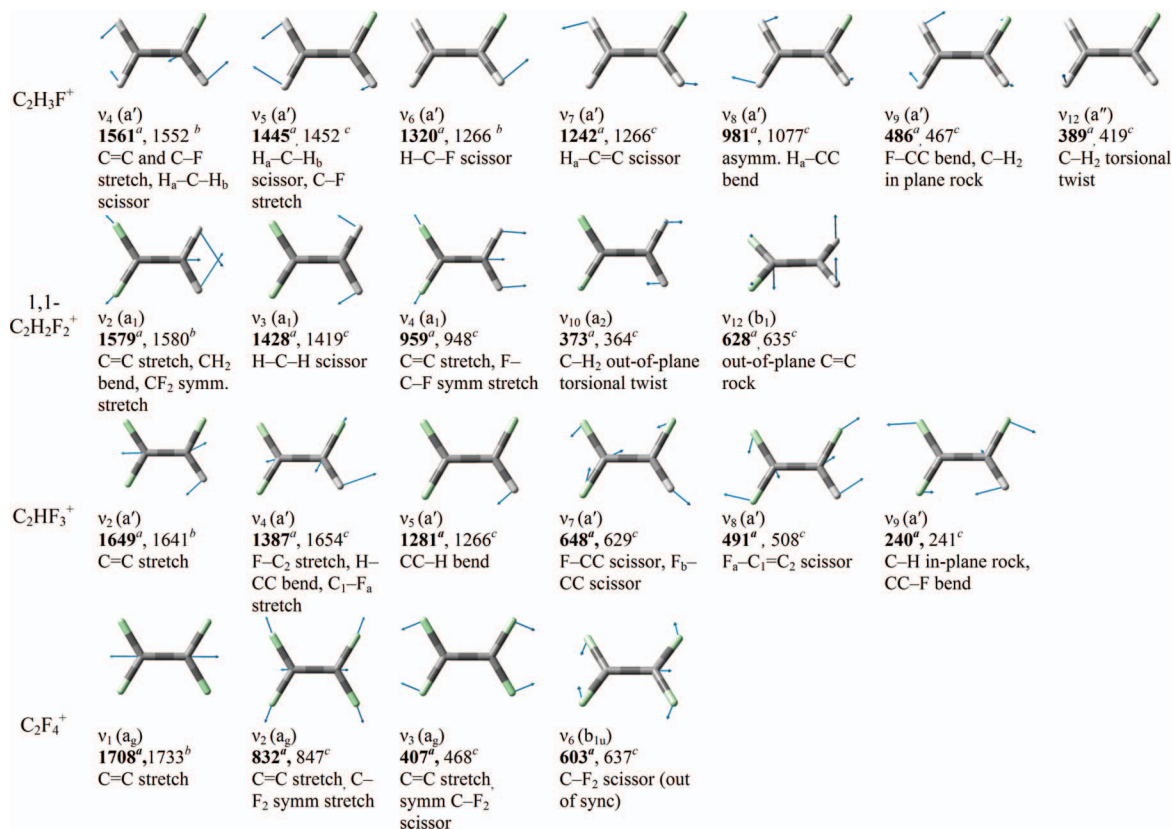
FIG. 2. Franck–Condon active vibrational modes of C$_2$H$_3$F, 1,1-C$_2$H$_2$F$_2$, C$_2$HF$_3$, and C$_2$F$_4$ upon ionization. [a]B3LYP/6–311++G(d,p) harmonic frequencies. [b]Harmonic frequencies derived by Morse-fitting of the vibrational progressions (see text). [c]Frequencies corresponding to the 1 ← 0 transition as observed in the TPES.

Franck–Condon simulation indicates that both ν_6, a H–C–F scissor and ν_7 contribute to the peak in the experimental spectrum. B3LYP calculates both vibrations to have a′ symmetry with vibrational wavenumbers of 1320 and 1242 cm^{-1}, respectively, to be compared with our experimental value of 0.157 eV or 1266 cm^{-1}. Comparison of the stick and the convoluted spectra suggests that ν_6 and ν_7 are indeed both blended in the peak at 10.523 eV. There was some ambiguity over the assignment of a weak peak at 10.498 eV.[5] It is comprised of two modes, ν_8 (a′) with $2\nu_9$ (a′), which are only 9 cm^{-1} apart with comparable Franck–Condon factors. In this instance, we can say with a degree of certainty that the assignment is not simply a matter of either ν_8 or $2\nu_9$, but both transitions are in fact present.

2. 1,1-Difluoroethene

Figure 1(b) shows the TPES of 1,1-$C_2H_2F_2$ together with the simulated stick and convoluted spectra. The $(2b_1)^2$ HOMO of the C_{2v} neutral corresponds to a cation ground state of $\tilde{X}\ ^2B_1$ symmetry. *Ab initio* calculations show there is a significant increase in the C=C bond length from 1.317 to 1.412 Å upon ionization, and a smaller decrease in the C–F bond length from 1.327 to 1.264 Å. The FCfit analysis results in a small twisting of the CF_2 group with respect to the CH_2 group upon ionization (i.e., the dihedral angle of F–C=C–H changes from 180° to 177°), thus the planarity of the molecule is lost in the ground state of the cation. For clarity, we retain the C_{2v} notation for the vibrational mode symmetries in the cation. Our spectrum agrees well with both the TPES recorded at lower resolution and the HeI PES recorded at a comparable resolution by Locht *et al.*[6] The AIE is 10.303 ± 0.005 eV, and the VIE is 10.496 ± 0.005 eV. The major vibrational progression has been assigned to the $n\nu_2$ (n = 0–6) C=C stretching mode of a_1 symmetry and the peak positions given in Table S5 of the supplementary material[26] are in excellent agreement with those of Locht *et al.*[6] Our value for the harmonic frequency ν_2 of 1580 cm^{-1}, obtained from Morse fitting of the progression, is in stunning agreement with the *ab initio* value of 1579 cm^{-1}. The anharmonicity constant, x_e, is determined to be 0.0046. Three further minor progressions are also identified and their peak positions are in reasonable agreement with the HeI study of Locht *et al.*[6] Vibrational assignments are given in Figure 1(b). For the sake of brevity, the *ab initio* frequencies, observed frequencies, and peak positions are given in Tables S5 and S6 of the supplementary material.[26]

There are several minor peaks sandwiched in between the ν_2 peaks of the main progression. The first one is observed at 10.348 eV and is best assigned to one quantum of ν_{10} (a_2) by FCfit. The experimental value of ν_{10} = 363 cm^{-1} is in agreement with the *ab initio* result of 373 cm^{-1}. Locht *et al.*[6] assign this peak to ν_9 (b_2), for which the calculated value of 417 cm^{-1} is much higher than the experimental value. It applies to both assignments, however, that these non-totally symmetric vibrations should be forbidden. A possible explanation of how ν_{10} is observed could be linked to the loss of planar symmetry upon ionization. Herzberg–Teller[30] vibronic

coupling between the $\tilde{X}\ ^2B_1$ and $\tilde{A}\ ^2B_2$ states of 1,1-$C_2H_2F_2^+$ which is mediated by the ν_{10} (a_2) twisting vibrational mode can occur, according to the symmetry requirement

$$\Gamma_e^{\tilde{X}} \otimes \Gamma_e^{\tilde{A}} \supset \Gamma_v. \qquad (1)$$

This requirement is satisfied here since the coupling of the vibronic symmetry of the $\tilde{X}$ and $\tilde{A}$ states, $B_1 \otimes B_2 = A_2$, gives the symmetry of the ν_{10} vibrational mode. Therefore, the $^2B_1$ and $^2B_2$ ion states are coupled when the molecule twists since the LUMO energy[17] is lowered and the HOMO is raised, and intensity is given to the ν_{10} mode upon ionization. As the predicted torsional angle is only ±3°, the double-minimum potential energy curve must be very shallow with the ν_{10} = 0 and 1 levels most likely above the barrier. In contrast, the non-adiabatic coupling (conical intersection) between the $\tilde{X}$ and $\tilde{A}$ states of $C_2H_4^+$, which is mediated by the torsional mode, produces a torsional angle at the minima of the ground state which is much larger, ±29°, with a barrier height of 357 cm^{-1}.[17] The difference in the extent of coupling and therefore the amount of twist seen could be due, in part, to the larger difference in energy[31] between the $\tilde{X}$ and $\tilde{A}$ states of 1,1-$C_2H_2F_2^+$ of 4.31 eV compared with that of $C_2H_4^+$ of 2.31 eV.[3]

The second of these minor peaks at 10.382 eV lies 637 cm^{-1} above the band origin and is also well reproduced in the Franck–Condon fitting by the ν_{12} mode of b_1 symmetry at 628 cm^{-1}. This is the only mode within 50 cm^{-1} of the experimental value of 637 cm^{-1}. Populating the F–C–F scissor ν_5 mode of a_1 symmetry with a frequency of 583 cm^{-1} gives a similar fit, but it is slightly lower in energy than the ν_{12} mode (see Figure S1 of the supplementary material).[26] The Franck–Condon simulation yields a third minor peak at 10.397 eV, which corresponds to a shoulder in the experimental spectrum at 10.394 eV, assigned as two quanta in the ν_{10} mode of a_2 symmetry (2 × 373 cm^{-1}). The difference between the band origin and this shoulder is 0.091 eV or 734 cm^{-1} which is close to the calculated value of 746 cm^{-1}. This mode becomes allowed under symmetry considerations even without the breakdown of planarity. Locht *et al.*[6] did not resolve this doublet and assigned the single peak as $2\nu_9$. Even if the HeI peak at 10.347 ± 0.004 eV had been correctly assigned as ν_9 by Locht *et al.*,[6] the 0.042 eV or 338 cm^{-1} spacing to the 10.389 ± 0.005 eV peak would still mean the latter is unlikely to be $2\nu_9$ with ν_9 = 417 cm^{-1}. We note that both the ν_{10} and ν_{12} modes involve a twisting of the CH_2 moiety which changes the dihedral angle, whereas the ν_9 mode consists of a F–CC asymmetric in-plane bend (wagging motion) between the CH_2 and CF_2 moieties which does not cause a change in this angle. When populating the ν_9 mode instead of either ν_{10} or ν_{12}, the resulting spectrum is not a satisfactory fit to the experimental spectra as the H–C=C angle of the cation becomes drastically reduced. In addition, the experimental spectrum cannot be faithfully reproduced when a planar cation geometry is retained, confirming that the twist gives rise to the observation of both the ν_{10} and ν_{12} modes.

The fourth peak to high energy of the origin band is at 10.420 eV. This is assigned to ν_4 (a_1) = 1, with this F–C–F symmetric stretching mode at 948 cm^{-1}, to be compared with

the *ab initio* value of 959 cm^{-1}. Finally, there is a partially resolved shoulder (starting at 10.479 eV) to lower energy of each peak of the main ν_2 (a_1) progression. Based on our simulation, this may correspond to the ν_3 (a_1) vibrational mode, observed experimentally at around 1418 cm^{-1}, which can be compared with the *ab initio* value of 1428 cm^{-1}. This progression was not observed by Locht *et al.*,[6] although the peaks in their ν_2 progression do appear to be slightly asymmetric. The same pattern of peaks due to the vibrational modes ν_{10}, ν_{12}, $2\nu_{10}$, ν_4, and ν_3 is repeated for members of the main progression of $n\nu_2$ ($n = 0–3$).

3. Trifluoroethene

Figure 1(c) shows the TPES of C_2HF_3, the simulated stick and convoluted spectra together with the vibrational assignments. Although some vibrational structure has been observed in the ground-state PE band by others,[1,3] this is the first high resolution TPES of this molecule reported in the literature. The $(4a'')^2$ HOMO of the neutral C_S C_2HF_3 molecule has C=C π orbital character, and the cation electronic ground state has the term symbol $\tilde{X}$ $^2A''$. Similarly with the previous fluorinated ethenes, *ab initio* calculations show an increase in the C=C bond length from 1.323 to 1.418 Å consistent with removing an electron from the C=C π orbital, and a decrease in all C–F bond lengths of ≈0.06 Å. The geometry obtained from FCfit shows planarity is retained within the ion.

The first photoelectron band, corresponding to the $\tilde{X}$ $^2A''$ ground state of $C_2HF_3^+$, is comprised of a series of sharp and well-defined peaks. The AIE and VIE are 10.138 ± 0.007 and 10.544 ± 0.007 eV, respectively. Previous literature values are scarce with the notable exception of the work by Bieri *et al.*,[1] who reported the AIE as 10.14 eV and the VIE as 10.62 eV, both in close agreement with our values. The band is dominated by a vibrational progression of $n\nu_2$ mode ($n = 0–5$) which corresponds to the C=C stretching mode. The Morse-fitted vibrational harmonic frequency of this band is determined to be 1641 cm^{-1}, which is in close agreement with the *ab initio* value of 1649 cm^{-1}. The anharmonicity constant, x_e, is determined to be 0.000781. This assignment is in agreement with the early angle-resolved photoelectron spectrum of Sell and Kuppermann[3] (Tables S7 and S8 of the supplementary material).[26] There are five other, less intense vibrational progressions amidst members of the ν_2 progression. With the aid of FCfit, they are assigned to ν_9 (C–H in plane rock and CC–F bend) at 241 cm^{-1}, ν_8 (F_a–C_1C_2 scissor, where F_a is *cis* to the hydrogen) at 508 cm^{-1}, ν_7 (F–CC scissor and F_b–CC scissor where F_b is *trans* to the hydrogen) at 629 cm^{-1}, ν_5 (C–H wag) at 1266 cm^{-1}, and ν_4 (F–C_2 stretch, H–CC bend and C_1–F_a stretch) at 1654 cm^{-1}. The overall agreement between experiment and fit is excellent. Figure 2 shows the calculated and experimental vibrational modes which are active upon ionization and their symmetries. All six active modes are of a' symmetry and satisfy selection rules. Furthermore, just as for monofluoroethene with C_S symmetry, no single quantum of a'' vibrational modes are observed, consistent with a planar cation. Unlike monofluoroethene, however, double quanta of a'' modes are not observed in trifluoroethene. The same pat-

tern of peaks due to the vibrational modes ν_9, ν_8, ν_7, ν_5, and ν_4 is observed towards higher energy from the main progression peaks $n\nu_2$ ($n = 0–4$).

4. Tetrafluoroethene

C_2F_4 has the highest symmetry of the four molecules studied, belonging to the D_{2h} point group. The HOMO of the neutral is the C=C π bonding orbital, $(2b_{3u})^2$, and the cation ground state has the term symbol $\tilde{X}$ $^2B_{3u}$.[1] Using FC-fit, the ground state geometry of the cation is confirmed to be planar, and only totally symmetric vibrations in the D_{2h} point group should be observed in the photoelectron spectrum. As previously, there is an increase in the C=C bond length of 0.096 Å, a decrease in the C–F bond length of 0.056 Å. Overall across the series, the increase in C=C bond length upon ionization becomes greater with increasing F-substitution, but the decrease in C–F bond length is reduced, in accordance with the perfluoro effect, i.e., σ molecular orbitals are strongly stabilized by mixing of the ethylene group orbitals with the electronegative F-atom σ orbitals. By contrast, the mixing and stabilization of the π orbitals is much smaller and so strong C–F π antibonding character dominates.[2]

The first photoelectron band seen in Figure 1(d) is assigned to the ground state of $C_2F_4^+$, $\tilde{X}$ $^2B_{3u}$. It is composed of several well-defined vibrational progressions, the most prominent being the $n\nu_1$ ($n = 0–7$), the C=C stretching mode at 1708 cm^{-1}, in good agreement with the experimental value from the Morse-fitted progression of 1733 cm^{-1}. The anharmonicity constant, x_e, is determined to be 0.00366. The calculated and experimental frequencies are given in Figure 2. The AIE and VIE are 10.110 ± 0.009 and 10.535 ± 0.009 eV, respectively. Five additional but less intense vibrational progressions are observed in between the members of the ν_1 progression. Three have been assigned as ν_3, ν_2, and ($\nu_3 + \nu_2$), with experimental frequencies of 468, 847, and 1315 cm^{-1}, respectively (see Figure 1(d)) and, as expected, all identified modes are of a_g symmetry (Tables S9 and S10 of the supplementary material).[26]

In an earlier lower resolution TPE study by Jarvis *et al.*,[7] only the ν_1, ν_2, and ν_3 modes were observed (note that the numbering of ν_1 and ν_2 is reversed in the studies of both Jarvis *et al.*[7] and Brundle *et al.*[2]). Following a subtraction procedure to allow for the effects of second-order harmonic radiation delivered from the grating monochromator at the beamline, Jarvis *et al.*[7] determined the AIE to be 10.0 ± 0.1 eV, and the vibrational frequencies of these three modes to be 1686, 766, and 371 cm^{-1}, in reasonable agreement with those determined from the present work of 1733, 847, and 468 cm^{-1}, respectively. The ground state of $C_2F_4^+$ was also studied by HeI photoelectron spectroscopy at a resolution of 0.022 eV by Eden *et al.*[8] The first and third progressions were also identified by Eden *et al.*[8] as ν_1 (C=C stretch) and ν_2 (C=C stretch and C–F_2 symmetric stretch). However, there is disagreement between the assignment of the second and fourth progression, which they assign by comparison with the infrared spectrum of neutral C_2F_4, as the ν_6 mode of b_{1g} symmetry and the ν_{11}

mode of b_{3u} symmetry using the Herzberg convention.[32] In the Mulliken convention used here, these vibrations are the ν_{11} (b_{3g}) CC–F bend and ν_5 (b_{1u}) symmetric C–F_2 stretch modes.[33] Since there is no change in the molecular symmetry, odd-quantum transitions are only allowed for totally symmetric modes. Therefore, we dispute the Eden[8] assignments to modes with b_{3g} and b_{1u} symmetry in favour of a combination band assignment where both modes have a_g symmetry. Consequently, we have reassigned these bands to be ν_3 and the combination band ($\nu_3 + \nu_2$), respectively. The average spacing between the second of the two peaks from the main progression is reported by Eden[8] as 0.152 eV or 1225 cm^{-1} and assigned to ν_{11}. However, the average difference in our work between this progression and the corresponding members of the ν_1 progression is 1245 cm^{-1}, but the difference between the band origin and the first member of this progression at 10.273 eV is 0.163 eV or 1315 cm^{-1}. This second value is least affected by anharmonicity and is preferred over the average value. It is also in excellent agreement with the sum of the experimental values for $\nu_3 + \nu_2$, 1315 cm^{-1}.

Thanks to the enhanced resolution, an additional, previously unobserved progression has been identified with two peaks in each member of the main progression with a spacing of 637 and 1008 cm^{-1} from the band origin. This progression with members at 10.188 and 10.235 eV is well reproduced when populating the ν_6 mode (C–F_2 scissor out of synchronicity) of b_{1u} symmetry with one and two quanta. Both the ν_6 mode and the other possibility, ν_9 of b_{2u} symmetry, are non-totally symmetric, so should be forbidden transitions in the absence of a geometry change upon ionization. Yet by evaluating the actual nuclear wave function overlap, Franck–Condon simulations show that ν_6 is populated with non-negligible intensity even without a change in symmetry. Finally, the same pattern of peaks at ν_2, ν_6, ν_3, $2\nu_6$, and ($\nu_2 + \nu_3$) is repeated for each member of $n\nu_1$ (n = 0–6).

It appears that with the exception of 1,1-$C_2H_2F_2^+$, the rest of the series studied in this paper, $C_2H_3F^+$, $C_2HF_3^+$, and $C_2F_4^+$ remain planar upon ionization in the ground electronic cation state. The experimental spectra cannot be faithfully reproduced with a non-planar ion geometry in these latter three ions. Apparently, the vibronic coupling between the π(C=C) and π(C–X_2) where X = H or F,[31] is only measurable in 1,1-$C_2H_2F_2^+$, in which a torsional twist is observed.

B. Electronically excited cation states

1. Spectroscopy

EOM-IP-CCSD/cc-pVTZ calculations were undertaken using Q-Chem 3.2[28] at the optimized G3B3 neutral geometries to determine accurate vertical ionization energies and assign excited electronic state TPES bands. Excited state wave functions of the cation are of single determinant character and the Koopmans' theorem[34] holds. Thus, the EOM-IP-CCSD assignment agrees exactly with the semi-empirical HAM/3-based ordering of the cations published 30 years ago by Bieri *et al.*[1] and, with the exception of the almost degenerate $\tilde{E}$, $\tilde{F}$ and $\tilde{H}$, $\tilde{I}$ electronic states in 1,1-$C_2H_2F_2^+$ and $C_2F_4^+$, respectively, also with their Green's function analy-
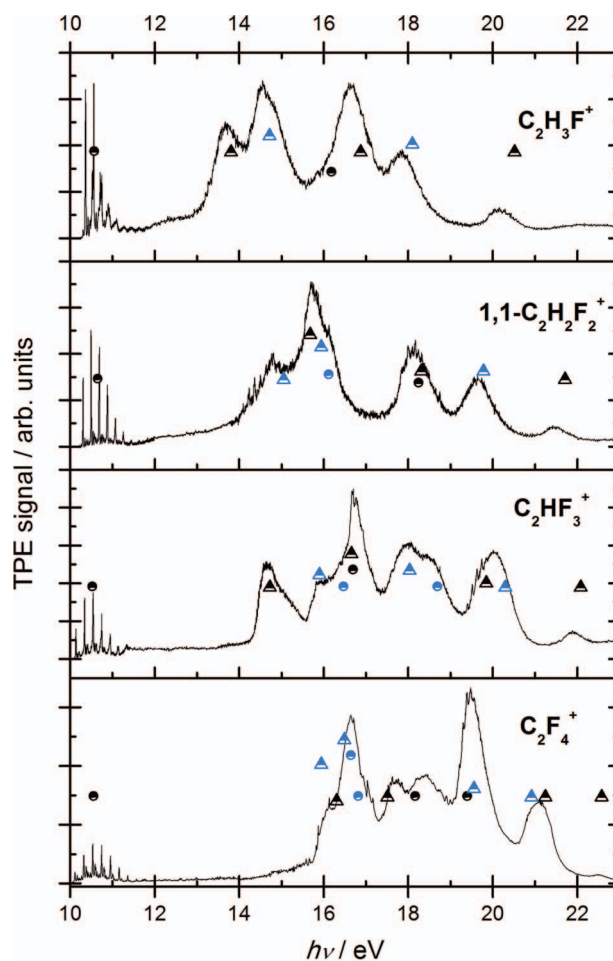

FIG. 3. Complete valence threshold photoelectron spectra of C_2H_3F, 1,1-$C_2H_2F_2$, C_2HF_3 and C_2F_4. The EOM-IP-CCSD/cc-pVTZ computed vertical ionization energies are shown by the symbols. Different symbols represent different ion states according to their (approximate, see text) C_{2v} character: A_1 (black triangle), A_2 (light circle), B_1 (black circle), B_2 (light triangle).

sis. Counter-intuitively, electronic excited state assignments are straightforward for the fluorinated ethene ions with little static electron correlation, in sharp contrast with the vibrational assignments of the ground state spectra, where we have found that even the most recent vibrational assignments need revision.[5,6,8]

Two of the molecules studied, C_2H_3F and C_2HF_3, have C_S symmetry, 1,1-$C_2H_2F_2$ has C_{2v} and C_2F_4 has D_{2h} symmetry. In order to establish trends and trace the evolution of the electronic ion states in the series, we considered the Kohn–Sham orbital character symmetries according to their C_{2v} character, even for the C_S molecules, as follows. Orbitals without a nodal plane along the C=C axis are classified as totally symmetric, giving the corresponding ion state A_1 symmetry. Ionization from orbitals with a nodal plane in the molecular plane but without one perpendicular to it leads to B_1 ion states. Orbitals with a nodal plane perpendicular to the molecular plane along the C=C axis correspond to B_2 ion states. When both nodal planes are present in orbitals, ionization leads to A_2 states. This assignment is shown together with the overall TPES in Figure 3. The slight destabilization of the π-type HOMO corresponding to the ground ion state

and the overall stabilization of the deeper lying orbitals, i.e., progressively higher ionization energies corresponding to excited ion states, with increasing F substitution confirms not only the perfluoro effect,[2] but also the enhanced stabilization of the fluorine lone pairs. With the exception of this point, other trends with increasing fluorine substitution are difficult to establish.

Vibrational progressions have been observed in some excited states in all four molecules. When vibrational structure is observed in the excited states, Franck–Condon factors have to be significant in the bottom of the potential energy well, and it can be assumed that the geometries of the excited state ion are comparable to that of the ground neutral state. Within this approximation, we make only tentative assignments based on the ion ground state calculated frequencies. A strong well-resolved progression is seen on the $\tilde{H}$ $^2A'$ state of $C_2HF_3^+$ between 19.4 and 20.3 eV which has not been previously reported. The observed spacing of $\sim$847 cm^{-1} could be attributed to an asymmetric wagging mode with a F_a–C_1F_b symmetric stretch, or even quanta of a F_a–C_1=C_2 bending mode. There is very weak vibrational structure seen between 22.5 and 24.9 eV with a separation of $\sim$240 cm^{-1}, which could be attributed to the CHF=CF$_2$ wagging mode. The strongest vibrational structure in the excited states of $C_2F_4^+$ is seen on the $\tilde{E}$ $^2B_{1g}$ peak at 17.6 eV, also observed in the HeI spectra of Brundle *et al.*[2] and Eden *et al.*[8] Brundle *et al.*[2] assign the complex structure to two separate progressions, ν_2 and ν_3. The ν_2 mode involving the C=C stretch, makes a more likely candidate for the major progression where we observe a vibrational spacing of $\sim$777 cm^{-1} rather than the ν_{11} mode (calculated at 536 cm^{-1} in the ground cation state) proposed by Eden *et al.*[8] The minor progression has an observed vibrational spacing of $\sim$398 cm^{-1} and we assign it to the ν_3 mode, a C=C stretch with symmetric C–F_2 scissor, in accordance with Brundle *et al.*[2] A final single vibrational progression is seen on the peak at 19.1–19.7 eV (ionic states with $\tilde{G}$ $^2B_{2g}$ and $\tilde{H}$ $^2B_{3u}$ symmetry) and is assigned to the ν_2 mode, $\sim$777 cm^{-1}, again in accordance with Brundle *et al.*[2]

2. Dynamics

The dissociative photoionization dynamics is of both applied and fundamental interest.[35] On the one hand, appearance energies can be used in thermochemical derivations, but only if the dissociative photoionization is fast at the thermochemical threshold[36] or if the dissociation rates can be measured and extrapolated to it.[37] In addition to new and accurate neutral thermochemistry, such thresholds can also help interpret the products of ion-molecule bimolecular reactions.[38] On the other hand, understanding the energy flow between different electronic and nuclear degrees of freedom is of paramount fundamental interest. A dissociation process in any molecular system (neutral or charged) is typically considered statistical if the intermediate state is sufficiently long-lived to allow for the complete redistribution of internal energy before dissociation. Such processes are dominated by the ground electronic state, since its density of states exceed that of any excited state by orders of magnitude.[35] Non-statistical, non-ergodic

processes are characterized by an incomplete sampling of the energetically allowed phase space of the dissociating species. The reason can be a fast dissociation process, such as impulsive F-loss from CF_4^+,[39] or Cl-loss from CCl_4^+.[40] Alternatively, an electronically excited ion state can be so long-lived that it establishes a second dissociation regime, shielded from access to the ground state dynamics of that surface. This was shown to be the case in F-atom loss in $C_2F_4^+$,[9] and probably applies in CH$_3$-loss from CH_3OH^+.[41] The nature of the non-statistical fluorine atom loss from singly to triply fluorinated ethene cations has long been misunderstood.[10–13] Contrary to F-loss from $C_2F_4^+$, detailed kinetic energy release studies have shown that F-loss from $C_2H_3F^+$ and 1,1-$C_2H_2F_2^+$ is, in part, an impulsive process.[11,42] The F-loss threshold ion yield curves were shown to correlate only approximately with the TPES signal,[9] which indicates a complex mechanism with possible Rydberg-state involvement. In contrast to $C_2F_4^+$, the state which leads unhindered to F-loss is not the first electronically excited state of the parent ion in the other members of the series. Intermediate Rydberg and ion states facilitate fast internal conversion and rule out long-lived electronically excited states. Therefore, non-statistical F-loss channels have to be fast and impulsive.

In the context of the overall valence TPES and experimental and computational information on excited electronic state energetics presented herein, it is now possible to stimulate the discussion on the unimolecular dissociation dynamics of fluorinated ethenes with respect to our previous study.[9] Out of computational practicality, we only address the dissociation mechanism of monofluoroethene cations by EOM-IP-CCSD/cc-pVTZ calculations along the optimized[9] cation ground electronic state H-, HF-, and F-loss reaction paths. That is, the reaction path geometries are optimized at the B3LYP/6-311++G(d,p) level on the ground cation state, and vertical excitations are considered to the electronically excited states. Because of the spectral similarity, we expect an analogous mechanism to apply to the dissociation dynamics of di- and trifluoroethene cations. By contrast, the spectral sparsity of the TPES of tetrafluoroethene leads to a de-coupling of the $\tilde{A}$ ion state from the $\tilde{X}$ ion state, and to isolated-state behaviour with long-lived $\tilde{A}$ state intermediates.[9] By understanding the role of different electronically excited ion states in the mechanism of the main dissociative photoionization channels, we will show how and why F-atom loss assumes a non-statistical character in higher internal energy states of the parent ions, whereas the HF- and H-loss channels do not.

a. H-atom loss from $C_2H_3F^+$. The H-loss reaction energy curves in the monofluoroethene cation are shown in Figure 4. The doublet ground ion state is of A'' symmetry. The molecular orbital of the missing electron in the dominant electron configuration of the $\tilde{X} - \tilde{C}$ states of the cation are shown in the figure, together with that in the ground state ion at an extended C–F bond length of 2.9 Å. The F atom is pointing out of the plane towards the reader in the schematic structures. The ground state of the H-loss fragment ion, CH$_2$=CF$^+$, is closed shell, i.e., totally symmetric (A') in C_S symmetry, and
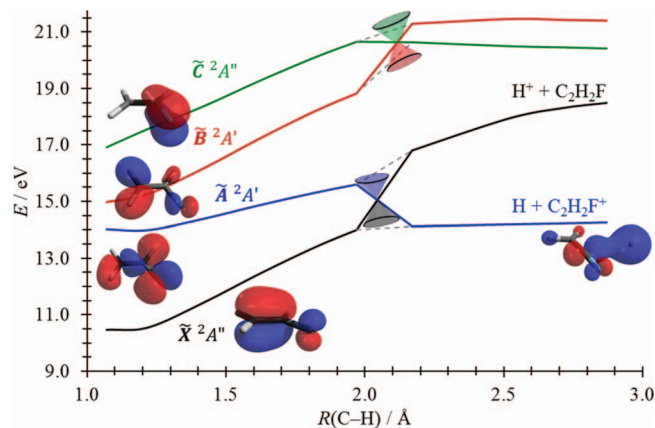
FIG. 4. Reaction curves of the $\tilde{X}$, $\tilde{A}$, $\tilde{B}$ and $\tilde{C}$ excited states of $C_2H_3F^+$ along the H-loss coordinate in the ground state ion. Conical intersections (indicated as funnels) are indicated at $R(C–H) \approx 2.05$ Å between the $\tilde{X}$ and $\tilde{A}$ states, and at $R(C–H) \approx 2.1$ Å between the $\tilde{B}$ and $\tilde{C}$ states.

FIG. 5. Reaction curves of the $\tilde{X}$, $\tilde{A}$, $\tilde{B}$ and $\tilde{C}$ excited states of $C_2H_3F^+$ along the HF-loss coordinate. A conical intersection has been located at $R(C\bullet C–H\bullet F) \approx 1.5$ Å.

the spin density is localized in the $1s$ orbital of the leaving H atom in the products. In other words, the $\tilde{X}$ state of the parent ion correlates adiabatically with the $CH_2=CF^{\cdot} + H^+$ dissociation products, but H^+ is not observed in the valence photoionization experiments.[9] The thermochemical threshold to H-atom loss is much lower at 13.6 eV.[9] In order to determine the well depth of the $\tilde{A}$ state, which can correlate adiabatically with the H-loss products, we carried out an EOM-IP-CCSD geometry optimization that yielded a structure with an elongated α-C–H bond length and increased C–C–F bond angle as well as an adiabatic ionization energy of 13.18 eV. Therefore, the $\tilde{A}$ state of $C_2H_3F^+$ is bound by ≈ 400 meV, it adiabatically correlates with the ground state H-loss products, and is coupled with the $\tilde{X}$ state through the C=C–F bend coordinate. Fast relaxation through this conical intersection leads to statistical H-loss with $k > 10^7$ s^{-1} at threshold. Contrary to the diabatic coupling coordinates in HF and F losses (see later), the coupling vibrational mode in this case is the C=C–F bending mode, and not the reaction coordinate. This explains the discontinuities in the potential energy curves plotted in Figure 4. In the ground electronic state constrained geometry optimizations, electronic state switching occurs at a value of the reaction coordinate where the new state is more stable even at the C=C–F bond angle of the old state. Thus, there is a discontinuity in this bond angle and the curve crossings do not correspond to a point along the seam of the conical intersection. Instead, the seam is only known to be located within the dashed lines. As also seen in Figure 4, the $\tilde{B}$ and $\tilde{C}$ states are also coupled by a conical intersection but are distinct from the $\tilde{X}$ and $\tilde{A}$ states. Thus, only the $\tilde{X}$ and $\tilde{A}$ states participate in the H-loss channel with the exit channel being the $\tilde{A}$ state.

   b. HF loss from $C_2H_3F^+$.   The HF-loss potential energy curves are shown in Figure 5. After the closed-shell neutral HF leaves, the spin density is localized in the π-system of the ethyne fragment ion. The reaction coordinate is taken as the distance between the midpoints of the C=C and H–F bonds, and, again, there appears to be a conical intersection at play at $R \approx 1.5$ Å. The potential energy curves cross smoothly,
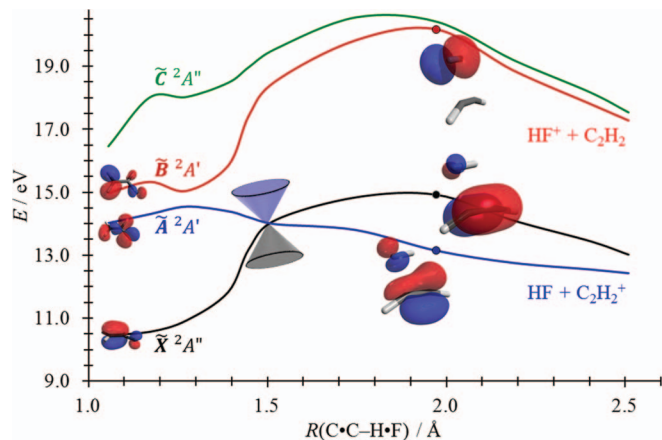
because the coupling vibrational coordinate is very similar to the reaction coordinate of choice. However, the $\tilde{X}$ $^2A''$ and $\tilde{A}$ $^2A'$ curves are degenerate at the dissociation limit ($R \gg 2.5$ Å, not shown in Figure 5), as they only differ in the orientation of the degenerate ethyne π-orbitals from which the electron is removed to form $C_2H_2^+$. As the products are approached, the (HOMO–1) of the neutral takes a σ-antibonding character between the fragments, whereas the HOMO corresponds to a π-antibonding orbital. Thus, at $R = 2.0$ Å, the A' state of the cation with one σ-antibonding electron removed is more stable than the A'' state ion (see schematic structures at the dots in the figure with the corresponding molecular orbitals in the neutral at the selected reaction coordinate with the HF leaving upwards). The energy difference between the two states is larger than 0.5 eV when HF is removed by 2.5 Å from $C_2H_2^+$, showing a long range interaction at play. The $\tilde{B}$ $^2A'$ state of $C_2H_3F^+$ correlates with the ground state $C_2H_2 + HF^+$ products, lying 5 eV above the lower energy $\tilde{X}$ and $\tilde{A}$ channels. The corresponding molecular orbital of the missing electron has F lone pair character, as shown. On the $\tilde{B}$ state surface, the transition state to HF loss lies 20 eV above the neutral, and is even higher for the $\tilde{C}$ and $\tilde{D}$ states which correlate with excited state products; the $\tilde{D}$ state is not shown in Figure 5. As was the case for H-atom loss, HF loss in $C_2H_3F^+$ is related to the interplay between the $\tilde{X}$ and $\tilde{A}$ states. Higher-lying ion states are de-coupled from the HF-loss channel observed in dissociative valence photoionization, as they must first relax to the $\tilde{X}/\tilde{A}$ manifold in order to lose HF in a statistical fashion.

   c. F-atom loss from $C_2H_3F^+$.   The F-loss potential energy curves, shown in Figure 6, show a different pattern. The first three ion states, $\tilde{X}$, $\tilde{A}$, and $\tilde{B}$, dissociate to products with different singly occupied fluorine $2p_{x,y,z}$ orbitals and the same ground electronic state of the $CH_2=CH^+$ ion. At a fluorine–carbon distance of around $R(C–F) = 2.3$ Å, the three states are degenerate and are coupled by the C–F stretch coordinate. At longer distances, the $\tilde{B}$ state appears to be converging to the dissociation limit, whereas even at $R = 3.3$ Å the $\tilde{X}$ and $\tilde{A}$ states are still increasing in energy. This suggests that long
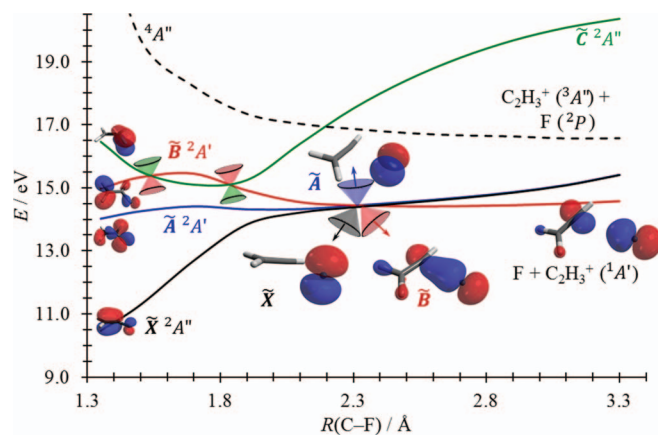
FIG. 6. Reaction curves of the $\tilde{X}$, $\tilde{A}$, $\tilde{B}$ and $\tilde{C}$ excited states of $C_2H_3F^+$ along the F-loss coordinate. Three conical intersections have been found $R(C–F) \approx 1.5$ Å between $\tilde{C}$ and $\tilde{B}$, $R(C–F) \approx 1.8$ Å between $\tilde{B}$ and $\tilde{C}$ and at $R(C–F) \approx 2.3$ Å between the $\tilde{X}$, $\tilde{A}$, and $\tilde{B}$ states leading to degenerate asymptotes.

range interactions are significant at even longer distances than for HF-loss, as there has to be an $\tilde{X}/\tilde{A}$ F-loss transition state at R(C–F) > 3.3 Å. To describe this bond length region reliably, the triple-ζ basis set used in these calculations would need to be augmented with several diffuse functions.

The non-statistical F-loss process arises in the energy range of the $\tilde{C}$ $^2A''$ state. Based on the low energy component in the kinetic energy release distribution and *ab initio* calculations, the dissociation channel from this $\tilde{C}$ state to the $C_2H_3^+$ ($^3A''$) + F (^2P) products was suggested to play an important role.[5,12,13] Roorda *et al.*[13] further established that the $\tilde{C}$ state has a large negative energy gradient towards the C–F elongation, and suggested a diabatic pathway in which the $\tilde{C}$ and $\tilde{X}$ states couple through an avoided crossing at $R(C–F)$ = 2.0 Å with a minimum energy gap of around 0.96 eV. They proposed that the route to F-atom formation is either via this diabatic pathway along which the initial momentum in the C–F stretch is retained, leading to ground state $C_2H_3^+$ ($^1A'$) with a large translational kinetic energy release, or via an adiabatic pathway along the $\tilde{C}$ state producing electronically excited triplet $C_2H_3^+$ ($^3A''$) fragment ion with small kinetic energy release. The fragments of the latter channel, however, correspond to a quartet wave function, meaning that it cannot be the asymptote of the doublet $\tilde{C}$ state. Indeed, we found that the $^4A''$ state crosses the $\tilde{C}$ $^2A''$ state at $R(C–F) \approx 2.2$ Å (Figure 6). The rate of intersystem crossing is unlikely to exceed that of internal conversion to lower lying doublet ion states and the breakdown diagram[9] casts further doubt on the feasibility of this pathway. The CBS-APNO[43] calculated splitting between the singlet and triplet states of the vinyl cation is 2.10 eV, putting the asymptote to triplet $C_2H_3^+$ production at $\approx$16.1 eV (cf. the 16.6 eV limit in Fig. 6 corresponding to the triplet energy at the singlet $C_2H_3^+$ product geometry, calculated using EOM-IP-CCSD/cc-pVTZ). In the breakdown diagram of $C_2H_3F^+$,[9] the percentage yield of F-loss production plateaus at $\approx$30% in the statistical regime, then rises rapidly in the photon energy region 15.5–16 eV to a constant level of $\approx$60% from which the signal decreases above a photon energy of 17.0 eV. If triplet $C_2H_3^+$ production were a viable dissociation path, the F-atom loss signal should increase above its

threshold at 16.1 eV, at which energy it has already reached its asymptotic value. The absence of such an increase rules out significant $C_2H_3^+$ ($^3A''$) production.

An alternative mechanism is now offered. As opposed to the $\tilde{X}$, $\tilde{A}$, and $\tilde{B}$ states, the $\tilde{C}$ state of $C_2H_3F^+$ converges to $CH_2CH + F^+$, and does not lead to F-loss products. However, it is just below the onset of this excited A'' ion state peak in the threshold photoelectron spectrum[9] that the non-statistical and partly impulsive[11] F-loss channel opens up. Figure 6 shows that the $\tilde{B}$ and $\tilde{C}$ states are coupled at 1.5 Å < $R(C–F)$ < 1.8 Å. As Roorda *et al.*[13] have shown, the C–F bond length in the $\tilde{C}$ state minimum is markedly longer than in the ground state of the ion, thanks to the removal of an electron from a π-type C–F bonding orbital. Consequently, $\tilde{C}$ state ions are highly vibrationally excited in the Franck–Condon envelope with large excitation in modes associated with the C–F stretch. They can lose electronic energy by crossing through the conical intersections to the $\tilde{B}$ state. If the crossing occurs at low C–F bond lengths on the bound part of the $\tilde{B}$ surface, the resulting species will decay statistically. However, at higher C–F bond lengths, the $\tilde{B}$ state also has a repulsive character that facilitates F-atom loss. The fate of the parent cation is still not sealed at this point, since fluorine p-orbital mixing at $R(C–F)$ = 2.3 Å can lead it onto the partially bound $\tilde{A}$ and $\tilde{X}$ states, yielding a longer lived F-loss intermediate in which redistribution of the excess energy may, to a certain extent, still be possible. Thus, three different F-loss channels are proposed in the $\tilde{C}$ state band of the TPES of C_2H_3F: (i) statistical F-loss mostly from the $\tilde{X}$ state by a $\tilde{C} \rightarrow \tilde{B}$ transition on the bound part of the $\tilde{B}$ state surface through the first conical intersection, (ii) impulsive F-loss by a $\tilde{C} \rightarrow \tilde{B}$ transition onto the repulsive part of the $\tilde{B}$ state and subsequent direct dissociation, and, as a slight variation of this process, (iii) semi-impulsive non-statistical F-loss by a multi-step $\tilde{C} \rightarrow \tilde{B} \rightarrow \tilde{X}/\tilde{A}$ transition with an intermediate at $R(C–F) \approx 2.3$ Å.

This multiple channel F-loss mechanism explains the proposed bimodal kinetic energy release distribution observed for $C_2H_3F^+$ and $1,1-C_2F_2H_2^+$,[12,13,42] as the low kinetic energy release modus is a result of the statistical dissociation pathway. Furthermore, direct $\tilde{C}$-state involvement is not necessarily required in threshold photoionization. In the CH_3I study,[22] it was proposed that the neutral parent can be excited to the Rydberg manifold in the initial step. The Rydberg manifolds belonging to each ion state will have the similar characteristics to the ion state, and autoionization may also occur after internal conversion. This explains why the non-statistical F-loss channel is seen at slightly lower energies than the actual $\tilde{C}$-state peak in the photoelectron spectrum of $C_2H_3F^+$. In the iodomethane study,[22] neutral dissociative states were proposed to connect different Rydberg manifolds with the corresponding ion states lying approximately 2 eV apart. In monofluoroethene, such neutral states do not need to be invoked, since the Rydberg manifolds themselves can readily interconvert at conical intersections. Such conical intersections may play a significant and, as yet, unrecognized role in ensuring that most molecules with a sufficiently congested ion spectrum dissociatively photoionize in accordance with statistical theory.[44]

IV. CONCLUSIONS

The ground state TPES of four fluorinated ethenes; C_2H_3F, 1,1-$C_2H_2F_2$, C_2HF_3, and C_2F_4 have been recorded at a higher resolution than previously reported. The ground state spectra have been simulated and fitted using the Franck–Condon fitting program, FCfit, to better identify those vibrational modes active upon ionization.[25] A number of weak peaks seen in the ground state band of $C_2H_3F^+$ have been reassigned. Even quanta transitions of the ν_{12} mode are allowed and $2\nu_{12}$ contributions have been identified. We have also reassigned vibrational transitions in the ground electronic state TPES of 1,1-$C_2H_2F_2$. In addition to the ν_2 C=C stretching mode previously observed by others, we identified the ν_3 mode which gives rise to asymmetry of all of the peaks in the ν_2 progression. The Franck–Condon analysis has also yielded a surprise result, revealing a small geometry change upon ionization, the loss of planarity. This led to the assignment of a non-symmetric ν_{10} (a_2) mode apparent in odd quanta. By contrast, Franck–Condon analysis shows that planar geometries in the monofluoroethene, trifluoroethene, and tetrafluoroethene ions are retained. The ground state TPES of C_2HF_3 has been recorded with significantly improved resolution than in previous studies. The ν_9, ν_8, ν_7, ν_5, and ν_4 vibrational progressions have been identified in addition to the ν_2 C=C stretching mode previously identified by Sell and Kuppermann.[3] Finally, the vibrational progressions in the C_2F_4 ground state TPES have been extensively re-assigned from the HeI study of Eden *et al.*[8] In addition to the strong C=C stretching mode $n\nu_1$ observed previously, we assign weak progressions to the ν_3, ν_2, and ($\nu_3 + \nu_2$) vibrational modes, all with a_g symmetry.

Excited state threshold photoelectron spectra are also reported for the four fluoroethenes up to 23 eV together with the computed vertical ionization energies. In contrast to the ground-state vibrational assignments, historical electronic state assignments have been found to be remarkably accurate. Based on excited state calculations on $C_2H_3F^+$ and new experimental data, we propose a new model for the non-statistical dissociative photoionization decay mechanism by F-atom loss as well as the previously observed bimodal F-loss kinetic energy release distribution. Triplet $C_2H_3^+$ fragment ion production by intersystem crossing is ruled out in the new mechanism, as is the isolated state mechanism proposed for F-loss from $C_2F_4^+$ in which the large separation of the electronic states slows down internal conversion. Instead, the $\tilde{C}$ $^2A''$ state of $C_2H_3F^+$ acts as a gateway with conical intersections to bound and dissociative parts of the $\tilde{B}$ state potential energy surface. Together with H and HF loss, statistical F-atom loss takes place via the $\tilde{X}$ state, whereas diabatic coupling onto the repulsive part of the $\tilde{B}$ state surface is responsible for non-statistical, impulsive F-loss.

[1]G. Bieri, W. V. Niessen, L. Åsbrink, and A. Svensson, Chem. Phys. **60**(1), 61 (1981).
[2]C. R. Brundle, M. B. Robin, N. A. Kuebler, and B. Harold, J. Am. Chem. Soc. **94**(5), 1451 (1972).
[3]J. A. Sell and A. Kuppermann, J. Chem. Phys. **71**(11), 4703 (1979).
[4]K. Takeshita, Theor. Chem. Acc. **101**, 343 (1999); Chem. Phys. **250**(2), 113 (1999).
[5]R. Locht, B. Leyh, D. Dehareng, K. Hottmann, and H. Baumgärtel, J. Phys. B **43**(1), 015102 (2010).
[6]R. Locht, D. Dehareng, and B. Leyh, J. Phys. B **45**(11), 115101 (2012).
[7]G. K. Jarvis, K. J. Boyle, C. A. Mayhew, and R. P. Tuckett, J. Phys. Chem. A **102**(19), 3230 (1998).
[8]S. Eden, P. Limão-Vieira, P. A. Kendall, N. J. Mason, J. Delwiche, M.-J. Hubin-Franskin, T. Tanaka, M. Kitajima, H. Tanaka, H. Cho, and S. V. Hoffmann, Chem. Phys. **297**(1–3), 257 (2004).
[9]J. Harvey, A. Bodi, R. P. Tuckett, and B. Sztáray, Phys. Chem. Chem. Phys. **14**, 3935 (2012).
[10]J. Dannacher, A. Schmelzer, J.-P. Stadelmann, and J. Vogt, Int. J. Mass Spectrom. Ion Phys. **31**, 175 (1979).
[11]F. Güthe, R. Locht, B. Leyh, H. Baumgärtel, and K.-M. Weitzel, J. Phys. Chem. A **103**(42), 8404 (1999).
[12]J. Momigny and R. Locht, Chem. Phys. Lett. **211**(2), 161 (1993).
[13]M. Roorda, A. J. Lorquet, and J. C. Lorquet, J. Phys. Chem. **95**(23), 9118 (1991).
[14]J.-L. Chang, C.-H. Huang, S.-C. Chen, T.-H. Yin, and Y.-T. Chen, J. Comput. Chem. **34**(9), 757–765 (2013).
[15]P. Hemberger, B. Noller, M. Steinbauer, I. Fischer, C. Alcaraz, B. R. K. Cunha de Miranda, G. A. Garcia, and H. Soldi-Lose, J. Phys. Chem. A **114**(42), 11269 (2010).
[16]L. Koziol, V. A. Mozhayskiy, B. J. Braams, J. M. Bowman, and A. I. Krylov, J. Phys. Chem. A **113**(27), 7802 (2009).
[17]S. Willitsch, U. Hollenstein, and F. Merkt, J. Chem. Phys. **120**(4), 1761 (2004).
[18]H. Köppel, L. S. Cederbaum, and W. Domcke, J. Chem. Phys. **77**(4), 2014 (1982); C. Sannen, G. Raşeev, C. Galloy, G. Fauville, and J. C. Lorquet, *ibid.* **74**(4), 2402 (1981).
[19]M. Johnson, A. Bodi, L. Schulz, and T. Gerber, Nucl. Instrum. Methods Phys. Res. A **610**, 597 (2009).
[20]A. Bodi, M. Johnson, T. Gerber, Z. Gengeliczki, B. Sztáray, and T. Baer, Rev. Sci. Instrum. **80**, 034101 (2009).
[21]B. Sztáray and T. Baer, Rev. Sci. Instrum. **74**(8), 3763 (2003).
[22]A. Bodi, N. S. Shuman, and T. Baer, Phys. Chem. Chem. Phys. **11**(46), 11013 (2009).
[23]W. A. Chupka, J. Chem. Phys. **98**(6), 4520 (1993).
[24]M. J. T. Frisch, G. W. Trucks, H. B. Schlegel *et al.*, GAUSSIAN 09, Revision A.1, Gaussian, Inc., Wallingford, CT, 2009.
[25]D. Spangenberg, P. Imhof, and K. Kleinermanns, Phys. Chem. Chem. Phys. **5**(12), 2505 (2003).
[26]See supplementary material at http://dx.doi.org/10.1063/1.4795428 for Tables S1–S10 and Figure S1.
[27]A. G. Baboul, L. A. Curtiss, P. C. Redfern, and K. J. Raghavachari, J. Chem. Phys. **110**(16), 7650 (1999).
[28]Y. Shao, L. F. Molnar, Y. Jung, J. Kussmann, C. Ochsenfeld, S. T. Brown, A. T. B. Gilbert, L. V. Slipchenko, S. V. Levchenko, D. P. O'Neill, R. A. DiStasio Jr., R. C. Lochan, T. Wang, G. J. O. Beran, N. A. Besley, J. M. Herbert, C. Y. Lin, T. V. Voorhis, S. H. Chien, A. Sodt, R. P. Steele, V. A. Rassolov, P. E. Maslen, P. P. Korambath, R. D. Adamson, B. Austin, J. Baker, E. F. C. Byrd, H. Dachsel, R. J. Doerksen, A. Dreuw, B. D. Dunietz, A. D. Dutoi, T. R. Furlani, S. R. Gwaltney, A. Heyden, S. Hirata, C.-P. Hsu, G. Kedziora, R. Z. Khalliulin, P. Klunzinger, A. M. Lee, M. S. Lee, W. Liang, I. Lotan, N. Nair, B. Peters, E. I. Proynov, A. Pieniazek, Y. M. Rhee, J. Ritchie, E. Rosta, C. D. Sherrill, A. C. Simmonett, J. E. Subotnik, H. L. Woodcock III, W. Zhang, A. T. Bell, A. K. Chakraborty, D. M.

Chipman, F. J. Keil, A. Warshel, W. J. Hehre, H. F. Schaefer III, J. Kong, A. I. Krylov, P. M. W. Gill, and M. Head-Gordon, Phys. Chem. Chem. Phys. **8**(27), 3172 (2006).

[29] P. M. Morse, Phys. Rev. **34**(1), 57 (1929).

[30] G. Herzberg and E. Teller, Z. Phys. Chem. Abt. B **21**, 410 (1933).

[31] H. Köppel, L. S. Cederbaurn, W. Domcke, and S. S. Shaik, Angew. Chem., Int. Ed. Engl. **22**(3), 210 (1983).

[32] T. Shimanouchi, *Tables of Molecular Vibrational Frequencies, Consolidated Volume I* (National Bureau of Standards, 1972), pp. 1–160.

[33] R. S. Mulliken, J. Chem. Phys. **23**(11), 1997 (1955).

[34] T. Koopmans, Physica **1**, 104 (1934).

[35] T. Baer, A. Guerrero, J. Z. Davalos, and A. Bodi, Phys. Chem. Chem. Phys. **13**(39), 17791 (2011).

[36] J. Harvey, R. P. Tuckett, and A. Bodi, J. Phys. Chem. A **116**(39), 9696 (2012).

[37] A. Bodi, M. D. Brannock, B. Sztáray, and T. Baer, Phys. Chem. Chem. Phys. **14**(46), 16047 (2012).

[38] M. J. Simpson and R. P. Tuckett, J. Phys. Chem. A **116**(31), 8119 (2012).

[39] I. G. Simm, C. J. Danby, J. H. D. Eland, and P. I. Mansell, J. Chem. Soc., Faraday Trans. 2 **72**, 426 (1976).

[40] D. M. Smith, R. P. Tuckett, K. R. Yoxall, K. Codling, and P. A. Hatherly, Chem. Phys. Lett. **216**(3), 493 (1993).

[41] S. Borkar, B. Sztáray, and A. Bodi, Phys. Chem. Chem. Phys. **13**(28), 13009 (2011).

[42] E. Gridelet, D. Dehareng, R. Locht, A. J. Lorquet, J. C. Lorquet, and B. Leyh, J. Phys. Chem. A **109**(37), 8225 (2005).

[43] J. W. Ochterski, G. A. Petersson, and J. A. Montgomery, J. Chem. Phys. **104**(7), 2598 (1996).

[44] T. Baer, B. Sztáray, J. P. Kercher, A. F. Lago, A. Bodi, C. Skull, and D. Palathinkal, Phys. Chem. Chem. Phys. **7**, 1507 (2005).